

Synthesis of Azobenzene-Containing Diblock Copolymers Using Atom Transfer Radical Polymerization and the Photoalignment Behavior

Li Cui and Yue Zhao*

Département de Chimie, Université de Sherbrooke, Sherbrooke, Québec, Canada J1K 2R1, and Centre de Recherche en Science et Ingénierie des Macromolécules (CERSIM), Université Laval, Québec, Canada G1K 7P4

Artashes Yavrian and Tigran Galstian

Centre d'Optique, Photonique et Lasers, Département de Physique, Université Laval, Ste-Foy, Québec G1K 7P4, Canada

Received August 7, 2003; Revised Manuscript Received August 28, 2003

ABSTRACT: A new series of liquid crystalline diblock copolymers composed of a polystyrene and a polymethacrylate with an azobenzene moiety in the side chain were synthesized through atom transfer radical polymerization and characterized by various techniques. Photoinduced birefringence of diblock copolymers and the azobenzene homopolymer was investigated and compared under different excitation conditions. The results show that the microdomain structures characteristic of diblock copolymers hinder the photoalignment of azobenzene mesogenic groups.

Introduction

Azobenzene-containing polymers are potentially useful materials for optical and photonic applications.^{1–7} Photoinduced trans–cis isomerization of the azobenzene chromophore and the possibility of orientation when irradiated with linearly polarized light are the properties exploited. Among the numerous amorphous and liquid crystalline azobenzene polymers investigated, random copolymers were frequently prepared.^{1,4,8,9} However, there are only few examples of block copolymers containing azobenzene moieties.^{10–12} Ober and co-workers developed a LC azobenzene block copolymer by linking azobenzene mesogenic groups to the isoprene block of a styrene–isoprene diblock copolymer prepared using living anionic polymerization.¹⁰ The group of Finkelmann reported the synthesis of azobenzene diblock and triblock copolymers through anionic polymerization.¹¹ More recently, Tian et al.¹² employed the atom transfer radical polymerization (ATRP) technique¹³ to prepare an amphiphilic diblock polymer composed of a hydrophilic poly(ethylene glycol) and an azobenzene LC block (lowest concentration: 86%).

Given the considerable interest generated by block copolymers that display a variety of microphase separation induced microdomain structures, more systematic studies on LC azobenzene block copolymers are obviously worth being conducted. In addition to the possible new morphologies in LC-coil diblock copolymers,^{10,14} the microstructures may affect the photochromic behavior of azobenzene groups.¹⁵ It is also conceivable that the photoisomerization of azobenzene may be used to influence the morphology or even the nanostructures that can self-assemble in block copolymers. In this paper, we report on the synthesis, by ATRP, of a new LC azobenzene diblock copolymer, namely poly{styrene-*b*-6-[4-(4-methoxyphenylazo)phenoxy]hexyl methacrylate}s. Since one of the most important properties of azobenzene polymers is the light-induced orientation of azobenzene

moieties, we have also investigated the photoinduced birefringence in the diblock copolymers and compared their behavior with the azobenzene homopolymer. As will be shown, the results revealed that the microdomain structures in diblock copolymers exert profound effects on the photoinduced alignment of azobenzene mesogenic groups.

Experimental Section

1. Synthesis. a. Materials. THF was refluxed with sodium and distilled. Styrene (purchased from Aldrich) was distilled with 2,6-di(*tert*-butyl-4-methyl)phenol as inhibitor before use. The other commercially available chemicals were used without further purification. The monomer for the LC azobenzene polymer, 6-[4-(4-methoxyphenylazo)phenoxy]hexyl methacrylate, was synthesized according to the method in the literature.¹⁶ Details on the preparation of all samples through ATRP are given below.

b. Preparation of the Homopolymer (PAzo). In a Schlenk flask, 3.46 mg of *N,N,N,N,N'*-pentamethyldiethylenetriamine (PMDETA, 0.02 mmol), 1.43 mg of CuBr (0.01 mmol), 100 mg of 6-[4-(4-methoxyphenylazo)phenoxy]hexyl methacrylate (0.25 mmol), and 0.4 mL of THF were charged and stirred for 30 min. 1.95 mg of ethyl bromoisobutylate (EBB, 0.01 mmol) was added, and immediately the mixture was frozen in with liquid nitrogen and a vacuum was applied. After several freeze–thaw cycles, the flask was sealed under vacuum and placed in an oil bath preheated at 60 °C; the reaction lasted 20 h. The solid formed was dissolved in THF and passed through an alumina column. Afterward, the polymer was precipitated in methanol several times. $M_n = 20\,840$ and $M_w/M_n = 1.23$ (GPC). It is noted that the molecular weight of PAzo is much higher than the calculated value based on the feed ratio of monomer/initiator. One possible explanation is that part of the initiator was not active in inducing polymerization of the azobenzene monomer. The difficulty of polymerizing azobenzene monomers through free radical polymerization has long been noticed.^{17,18}

c. Preparation of Macroinitiator Polystyrene–Br (PS–Br). In a Schlenk flask, 31.2 mg of 2,2-dipyridine (dPy, 0.2 mmol), 14.3 mg of CuBr (0.1 mmol), and 4.16 g of styrene (40 mmol) were charged and stirred for 30 min. 78 mg of ethyl bromoisobutylate (EBB, 0.4 mmol) was added, and immediately the mixture was frozen in with liquid nitrogen and a

* Corresponding author: e-mail Yue.Zhao@USherbrooke.ca.

Table 1. Characteristics of Synthesized Polymers

sample	azo block content (wt %)	M_n (NMR)	M_n (GPC)	M_w/M_n (GPC)	phase transitions ^a (°C)	ΔH_{S-N}^b (J/g)	ΔH_{N-I}^b (J/g)
PAzo	100		21K	1.23	g74S92N134I	2.25	2.75
P1	86	67K	58.1K	1.5	g72S90N128I	1.86	2.44
P2	80	42K	37.6K	1.29	g68S86N125I	1.81	2.39
P3	74	36K	33.4K	1.26	g67S85N122I	1.56	1.82
P4	57	21.8K	21.5K	1.26	g61S74N105I	0.76	0.96
P5	47	17.7K	16.1K	1.26	g60N112I		0.22
PS-Br	0		8380	1.25	g58I		

^a g = glass transition; S = smectic A phase; N = nematic phase; I = isotropic phase. ^b With respect to the LC block.

vacuum was applied. After several freeze–thaw cycles, the flask was sealed under vacuum and put in an oil bath at 100 °C for 20 h. The content was dissolved in chloroform and passed through an alumina column to remove the metal complex. After being concentrated, the chloroform solution was precipitated in methanol. The precipitation was repeated three to five times. The final product was dried at 50 °C under vacuum. $M_n = 8380$ and $M_w/M_n = 1.25$ (GPC).

d. Preparation of Block Copolymer P1. A round-bottom flask with a stir bar was charged with 50 mg of PS-Br as macroinitiator, 450 mg of 6-[4-(4-methoxyphenylazo)phenoxy]hexyl methacrylate, 20.9 mg of PMDETA, and about 0.5 mL of THF. The mixture was stirred for 20 min until a homogeneous solution was formed. 7.3 mg of copper bromide was then introduced, and three freeze–pump–thaw cycles were performed. The flask was sealed in freezing state under vacuum and put in an oil bath at 60 °C for 6 h. Conversion is determined as 72% by ¹H NMR. The reaction mixture was dissolved in chloroform and passed through an alumina column. The solution was concentrated, and finally the product was purified by repeated precipitation in methanol. Other block copolymers of different compositions (Table 1) were prepared using similar procedure.

2. Characterizations. ¹H NMR spectra were recorded on a Bruker spectrometer (250 MHz, AC 250). Molecular weights and polydispersities were measured by gel permeation chromatography (GPC) using a Waters system equipped with a refractive index and a photodiode array detector; THF was used as eluent (elution rate: 0.5 mL/min), and polystyrene standards were used for calibration. Textures were examined on a Leitz DMR-P polarizing microscope equipped with an Instec hot stage. Transition temperatures were measured using Perkin-Elmer DSC-7 differential scanning calorimeter (heating and cooling rates: 10 °C min⁻¹). UV–vis spectra were recorded with a HP 8452A spectrophotometer. Transmission electron microscope (TEM) observations were carried out on a Hitachi H-7000 instrument, operated at 75 kV. Thin films of about 50 nm were exposed to RuO₄ vapor for hours to stain the PS block.

3. Photoisomerization and Photoinduced Birefringence. Irradiation of the samples was performed using an UV and visible spot curing system (Novacure 2100) combined with UV and visible interference filters (10 nm bandwidth, Oriel). The intensity of the UV beam at $\lambda = 360$ nm was about 10 mW/cm², and that of the visible beam at $\lambda = 440$ nm was about 5 mW/cm². For the measurement of photoinduced birefringence, an optical setup similar to that described elsewhere¹⁹ was utilized. Basically, the sample (thin film of about 10 μ m thick prepared from solution casting) was placed between two crossed polarizers. An Ar⁺ ion laser ($\lambda = 488$ nm) was used as the excitation beam, whose propagation direction made a small angle to the normal to the film plane. The intensity of the excitation beam was adjusted to be 25 mW/cm², and the polarization was set to be 45° with respect to the crossed polarizers. A He–Ne laser ($\lambda = 633$ nm, 4 mW) was used as the probe light, with normal incidence. A photodiode detector behind the crossed polarizers monitored the transmission of the probe light. Any anisotropy due to the alignment of azobenzene groups when illuminated with the excitation beam would result in changes in transmission of the probe light, which can be measured and used to calculate the photoinduced birefringence.¹⁹ For all measurements, a second photodiode

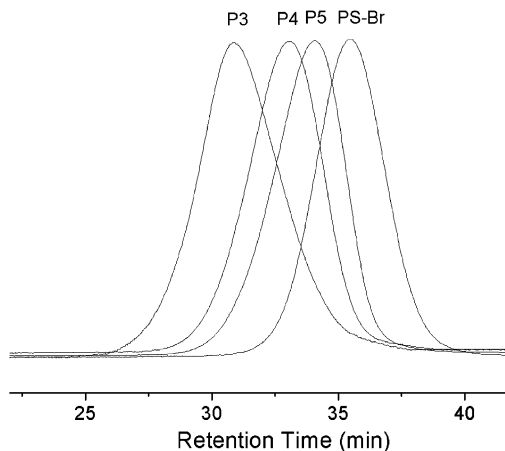


Figure 1. GPC curves of the PS-Br macroinitiator, $\bar{M}_n = 8.38 \times 10^3$ and $\bar{M}_w/\bar{M}_n = 1.25$, and the resulting block copolymers poly{styrene-*b*-6-[4-(4-methoxyphenylazo)phenoxy]hexyl methacrylate}s, P3, $\bar{M}_n = 3.76 \times 10^4$ and $\bar{M}_w/\bar{M}_n = 1.26$, P4, $\bar{M}_n = 2.15 \times 10^4$ and $\bar{M}_w/\bar{M}_n = 1.26$, and P5, $\bar{M}_n = 1.61 \times 10^4$ and $\bar{M}_w/\bar{M}_n = 1.26$.

detecting changes in intensity of the probe light before passing the second polarizer was used to make sure that the measured transmission changes were not caused by scattering or absorption of the sample.

Results and Discussion

1. Block Copolymerization through ATRP. ATRP has proved to be a very powerful polymerization technique for the preparation of block copolymers from a wide variety of monomers.^{20,21} In this work, a polystyrene (PS) macroinitiator was used to polymerize the azobenzene methacrylate monomer. The PS-Br macroinitiator was first prepared²² and its degree of activity examined by extension polymerization of styrene. GPC measurements indicated that the PS sample with extended molecular weight had a narrow polydispersity, showing no bimodality and containing little residual macroinitiator. This control experiment confirmed the efficient extension polymerization conditions using the PS-Br macroinitiator. The macroinitiator was then used to polymerize the azobenzene monomer, 6-[4-(4-methoxyphenylazo)phenoxy]hexyl methacrylate, to make the LC azobenzene block. The GPC curves in Figure 1 indicate a successful initiation and growth of the second block. Diblock copolymers with various contents (or volume fractions) of the LC azobenzene methacrylate block can readily be obtained by controlling the conversion and/or the amount of azobenzene monomer added for the extension polymerization. Most block copolymers prepared have a polydispersity similar to that of the PS macroinitiator (~1.25). Figure 2 shows the ¹H NMR spectrum for one of the diblock copolymers, P3. From the peak assignments, the composition of the diblock copolymer can easily be calculated. Thus, using the

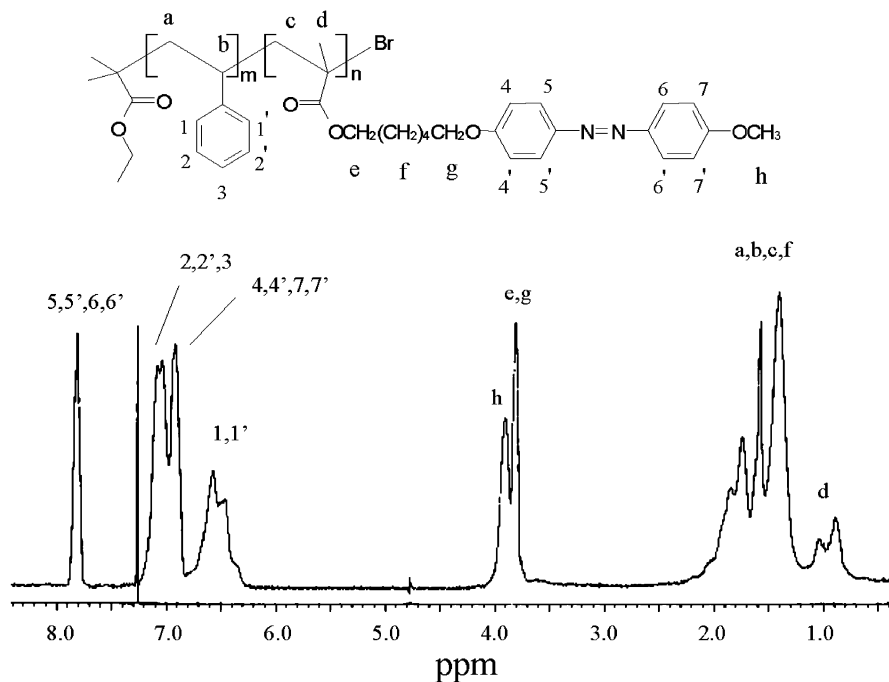


Figure 2. ^1H NMR spectrum of the diblock copolymer P3.

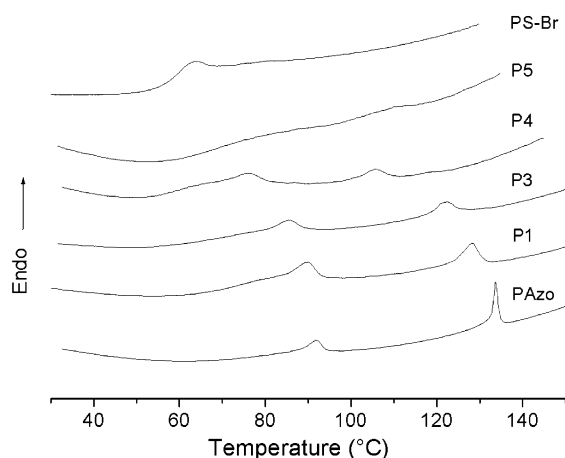


Figure 3. DSC heating curves of block copolymers and homopolymers.

GPC-determined $\bar{M}_n = 8380$ for the PS block, the number-average molecular weight of the diblock copolymer could be estimated from ^1H NMR. The results for all copolymers are summarized in Table 1 and compared to \bar{M}_n from GPC measurements using PS standards. Similar molecular weights were yielded from the two methods.

2. Phase Transition Behaviors and Morphology.

The phase transitions of the diblock copolymers were investigated by means of DSC and polarized optical microscopy. Figure 3 compares the second DSC heating curves of the block copolymers with the homopolymers, i.e., the PS macroinitiator and PAzo. On one hand, like the LC azobenzene homopolymer, the azobenzene block of all copolymers displays a smectic–nematic and a nematic–isotropic phase transition endotherm, with the exception of P5, which has the lowest azobenzene polymer content. P5 shows only one mesophase transition, presumably nematic–isotropic, near 112 °C. Since PAzo is known to have a smectic A phase,¹¹ the smectic phase in the block copolymer should be the same. On the other hand, the copolymer P1, which has the highest

azobenzene polymer content, has lower phase transition temperatures than PAzo, even though its azobenzene polymer block has a much higher molecular weight than the azobenzene homopolymer (Table 1). Such a decrease in thermal stability of the mesophases should be caused by the microdomain structure of the diblock copolymer and the effect of mixing with the PS block. Comparing the copolymers, as the fraction of azobenzene block decreases, the mesophase transitions as well as the T_g are generally shifted to lower temperatures (Table 1). Since they all have the same PS block, this reduction would be mainly explained by a molecular weight effect of the azobenzene polymer. The phase transition enthalpies are also reduced when the azobenzene polymer content is below 70%. The apparently quite low smectic–nematic phase transition enthalpy in the diblock copolymer may be indicative of a reduced smectic order within the microdomains. Note also that the values of ΔH_{S-N} in Table 1, measured from the phase transition peak, may contain appreciable errors due to the interference of the glass transition.

The mesophases in diblock copolymers were also observed on polarizing microscope. They exhibit significant differences as compared with the azobenzene homopolymer PAzo, in both the LC texture and the time required for the texture to develop. Figure 4 shows examples of polarizing optical micrographs for PAzo and three block copolymers, taken at temperatures slightly below their T_{ni} . In the case of PAzo, a nematic texture with dark threads was visible by cooling the sample from the isotropic phase, without any thermal annealing (Figure 4a). By contrast, block copolymers needed to be annealed for several minutes to have the texture developed, and the annealing times were longer for copolymers with a lower fraction of azobenzene block. With 86% azobenzene block, P1 shows a nematic texture with no dark threads (Figure 4b), while with 74% azobenzene block, P3 displays a texture with more fine grains (Figure 4c). When the fraction of azobenzene block is reduced to 47% for P5, only birefringent spots could be observed after 40 min annealing, which is

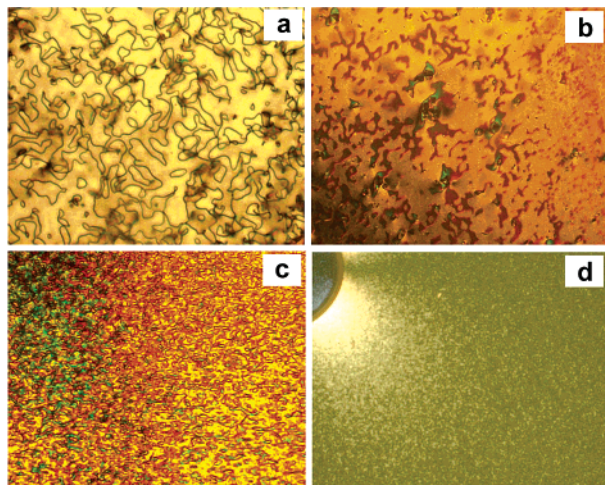


Figure 4. Polarizing optical micrographs for (a) PAzo (128 °C, 100 \times), (b) P1 (120 °C, 100 \times), (c) P4 (100 °C, 200 \times), and (d) P5 (96 °C, 100 \times).

consistent with the DSC measurements showing no prominent transition peaks for the sample cooled from the isotropic phase. These results imply that the microdomain structure in the diblock copolymer may render the arrangement of the mesogenic groups more difficult to develop.

The morphologies of these diblock copolymers were difficult to observe using TEM. The contrast of the domains could be brought out only after several days of annealing of the sample and hours of staining of thin films by RuO₄ vapor. Figure 5 shows the TEM images of two copolymers. For P3 with 74% azobenzene block, despite the image quality, some end-view cylinders of the PS domains are noticeable. For copolymers with a lower content of the azobenzene block, such as P4, the expected alternating lamellar morphology is observed.

3. Photoisomerization and Photoinduced Alignment. Photoinduced *trans*–*cis* isomerization of azobenzene mesogens was observed for solutions and films of PAzo and all diblock copolymers. As an example, Figure 6 compares the UV–vis spectra in the solid state of PAzo, P3, and P5, before and after UV exposure at 360 nm, reaching the photostationary state. In all cases, the UV irradiation lowers the absorption at 365 nm (π – π^* transition of *trans*-azobenzene) while raising the absorption around 450 nm (n – π^* transition of *cis*-azoben-

zene). It can be noted that the percentage of *cis*-azobenzene at the photostationary state, estimated from $\% \text{ cis} = 100(A_0 - A_s)/A_0$, where A_0 and A_s being the absorbance at 365 nm before and after irradiation, seems to increase with decreasing the concentration of the azobenzene block. It changes from about 52% for PAzo to 78% for P5.

Since the wavelength $\lambda = 488$ nm of the Ar⁺ ion laser used to induce the alignment of azobenzene groups is far from the absorption maximum of *trans*-azobenzene (365 nm) but close to the absorption band of *cis*-azobenzene (~ 450 nm, n – π^* transition), we investigated two ways to induce the alignment of azobenzene. In one, the excitation beam was applied to the as-cast films that mainly contain *trans*-azobenzene, while in the other, the films were preirradiated with an unpolarized UV lamp to obtain the *cis*-rich state before application of the excitation laser. The results of photoinduced birefringence in PAzo, P3, and P5 under the two conditions are presented in Figure 7. All films prior to exposure already show a small birefringence of about 0.001–0.002, and this birefringence is normalized to zero to better compare the growth of the photoinduced anisotropy. Two observations can be made. On one hand, with or without the preirradiation of UV light, the photoinduced birefringence of diblock copolymers is smaller than that of the homopolymer PAzo, and it decreases with decreasing the fraction of the azobenzene block. The differences in birefringence cannot be explained only by the different fractions of the azobenzene block (74% in P3 and 47% in P5); rather, they would reflect the effects of microdomain structures in block copolymers on the photoalignment of azobenzene. On the other hand, for all polymers, the photoinduced birefringence is significantly higher for the film subjected to the UV preirradiation. This implies different mechanisms for the azobenzene alignment with the *trans*-rich and *cis*-rich states prior to irradiation.

To get more insight into the mechanisms, we also performed photoinduced birefringence measurements with much longer irradiation times. The typical results are shown in Figure 8 with the block copolymer P3 as example. For the film preirradiated with UV light, the birefringence develops more quickly, and there are clearly two distinct mechanisms involved in the process. When the excitation beam is on, the birefringence rises first exponentially within the first 200 s, and then it

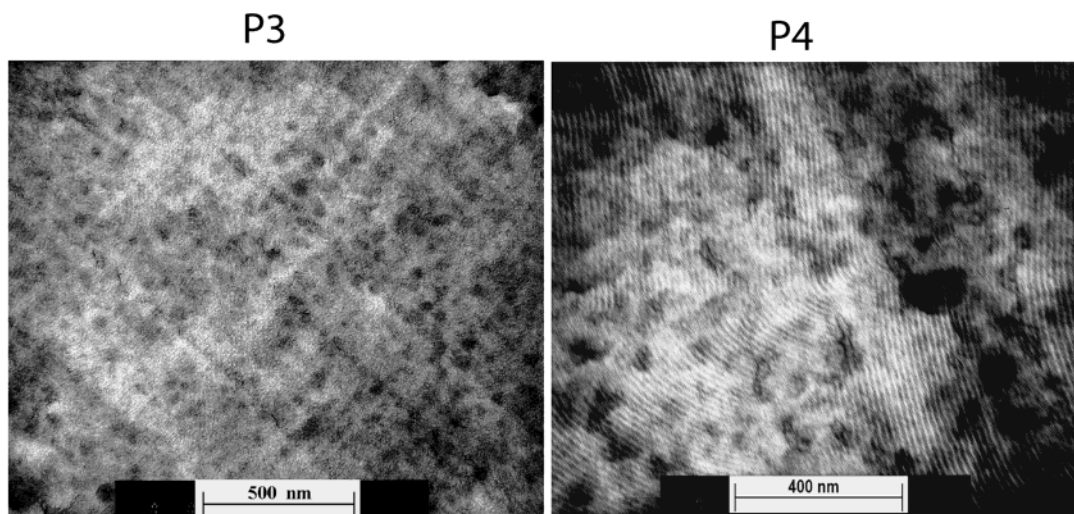


Figure 5. TEM images of diblock copolymers.

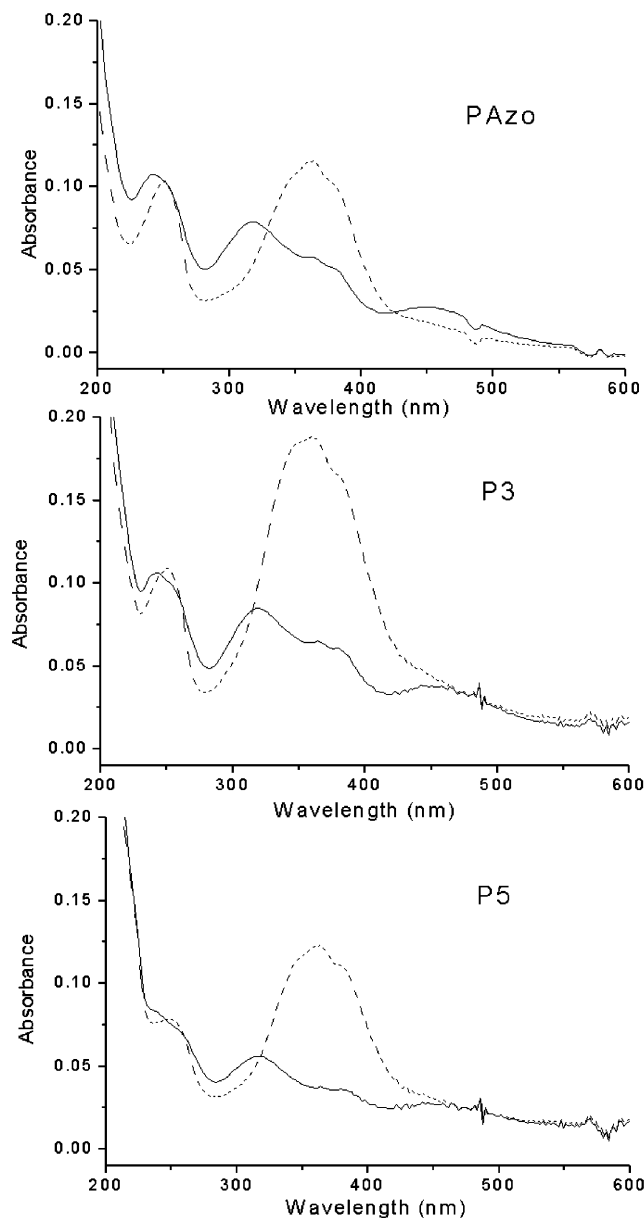


Figure 6. UV-vis spectra of PAzo, P3, and P5 in the solid state before (dotted lines) and after UV exposure at 360 nm (solid lines) reaching the photostationary state.

seems to stabilize toward a plateau value. However, at longer times, >300 s, the birefringence goes up again in an almost linear fashion, with a slope similar to the curve for the film without preirradiation of UV light. The same birefringence level can be achieved in the film with no preirradiation, but it takes much longer irradiation time. Also noticed from Figure 8 are (1) for both films only a very slight relaxation in birefringence occurs when the excitation beam is turned off; (2) as revealed by the film with no preirradiation, when the irradiation intensity is increased from 25 to 50 mW/cm^2 the increase in birefringence is faster; and (3) circularly polarized light effectively erases the birefringence induced in the film with no preirradiation, while for the preirradiated film, it can only erase a fraction of the birefringence, which apparently is the fraction induced after 300 s.

On the basis of the above results, we suggest the two scenarios schematically depicted in Figure 9. On one hand, for the as-cast film with no UV preirradiation, it

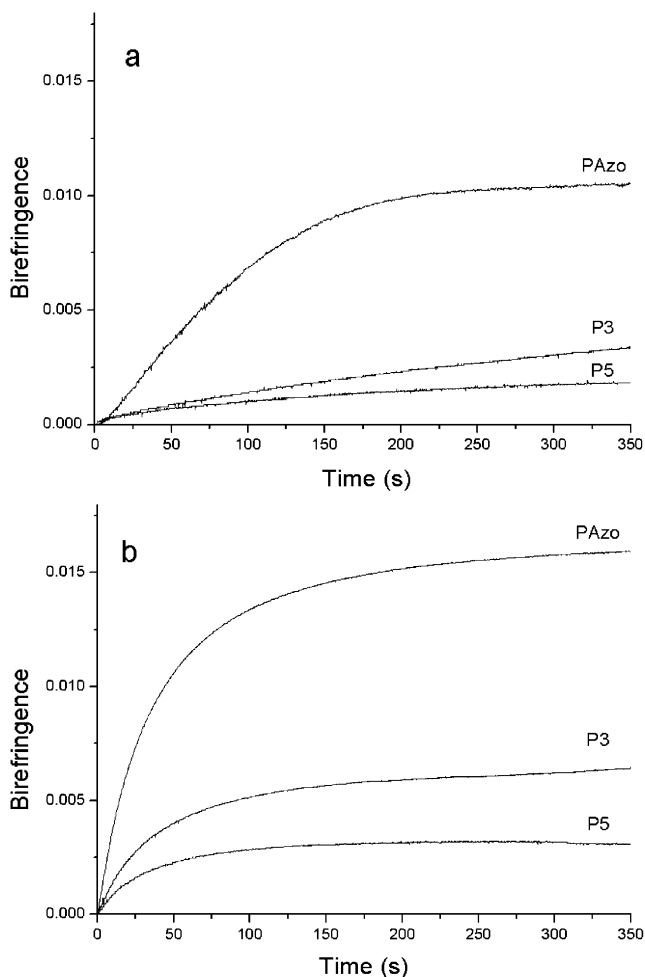


Figure 7. Photoinduced birefringence of PAzo, P3, and P5 on laser excitation at 488 nm: (a) as-cast films; (b) films preirradiated with UV light to reach the photostationary state rich in *cis* form.

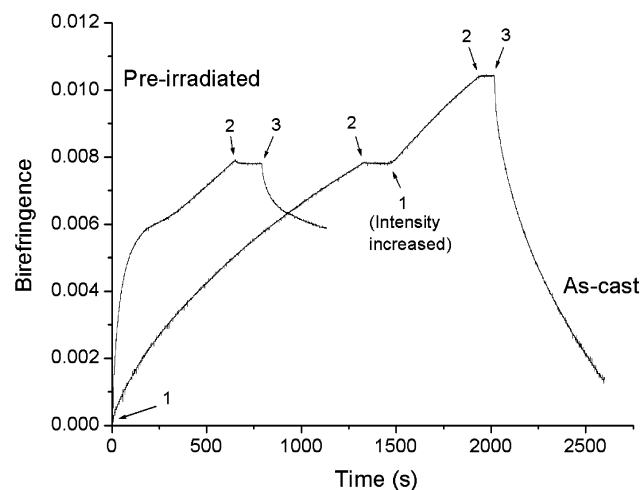


Figure 8. Stability of photoinduced birefringence of P3: (1) excitation laser is on, (2) laser turned off, and (3) circularly polarized laser is on. See text for details.

has *trans*-azobenzene groups. Under linearly polarized irradiation at 488 nm, a small fraction of azobenzene groups may undergo the *trans*-*cis* isomerization. As 488 nm is close to the absorption band of *cis*-azobenzene, the *cis*-*trans* back-isomerization is likely to be activated by the irradiation light. This should lead to repeat cycles of *trans*-*cis* and *cis*-*trans* photoisomerization, which is

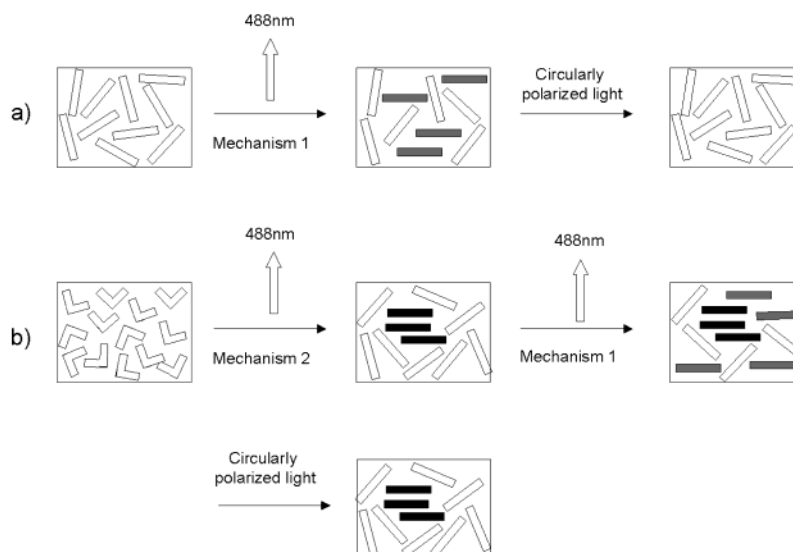


Figure 9. Schematic illustration of the proposed photoalignment mechanism for (a) as-cast film and (b) film preirradiated with UV light.

known to induce orientation of *trans*-azobenzene perpendicular to the polarization of the excitation beam.¹ The birefringence increases slowly because the excitation wavelength is far from the maximum absorption of *trans*-azobenzene. This process is referred to as mechanism 1. The fact that the birefringence can be readily erased by circularly polarized light implies that the oriented *trans*-azobenzene groups are in an amorphous-like state. On the other hand, for the film preirradiated with UV light, it contains more *cis*-azobenzene. On irradiation, a large fraction of the *cis*-azobenzene groups should be activated and converted to *trans*-azobenzene. This fast process, denoted as mechanism 2, would result in *trans*-azobenzene groups that are preferentially aligned normal to the polarization of the excitation beam and account for the quick early increase in birefringence. At a certain irradiation time, the photostationary *trans*-rich state is recovered, and for the *trans*-azobenzene groups that are not yet aligned perpendicularly to the excitation polarization, the situation is the same as for the film with no preirradiation. That is, mechanism 1 becomes the dominant process and increases the birefringence over time. Not sketched in Figure 9 is the portion of *trans*-azobenzene remained after the preirradiation with UV light; these molecules also respond to the laser excitation following mechanism 1. The fact that circularly polarized light cannot remove the birefringence induced by mechanism 2 suggests that the oriented *trans*-azobenzene groups form liquid crystalline domains that are known to be difficult to randomize.¹ This is possible because the preirradiation with UV light, resulting in *cis*-azobenzene groups in the film, has a similar effect to the photochemical phase transition into the isotropic phase,⁸ which might facilitate the formation of liquid crystalline domains by oriented *trans*-azobenzene groups.

It is worth discussing the possible effects of the microdomain structures in diblock copolymers on the photoinduced alignment of azobenzene groups. As mentioned above, Figure 7 shows that the smaller birefringence of diblock copolymers cannot be accounted by the dilution effect. Indeed, the copolymer P3 has 74% azobenzene block, but its birefringence after 350 s is about a third of that of the homopolymer PAzo without preirradiation with UV light and 40% with preirradia-

tion. While for P5, which has 47% of azobenzene block, its birefringence is only about 17 and 19% of that of PAzo in the two cases. These results imply that the photoinduced orientation of azobenzene groups may be more difficult to develop in the diblock copolymers than in the homopolymer. For both the microphase-separated lamellar morphology (P5) and the morphology with PS cylindrical domains dispersed in the azobenzene polymer matrix (P3), the azobenzene groups are constrained due to the microdomain structures, being confined either inside the lamellae or between the PS cylinders as the distance between cylinders is in the order of tens of nanometers.¹⁰ These constraints may hinder the development of photoinduced alignment of azobenzene groups.

Conclusions

Atom transfer radical polymerization was employed to prepare a diblock copolymer composed of polystyrene and a liquid crystalline azobenzene-containing polymethacrylate, yielding samples with various compositions and narrow polydispersity. Photoinduced birefringence measurements revealed that under different excitation conditions azobenzene mesogenic groups confined in the microdomain structures of the diblock copolymer respond to light differently than the azobenzene homopolymer. The microdomains hinder the photoalignment of azobenzene.

Acknowledgment. We thank Dr. X. Yan and Prof. G. Liu (University of Calgary) for the TEM observation. Financial support from the Natural Sciences and Engineering Research Council of Canada and le Fonds québécois de la recherche sur la nature et les technologies of Québec is also acknowledged.

References and Notes

- (1) Natansohn, A.; Rochon, P. *Chem. Rev.* **2002**, *102*, 4139.
- (2) Ikeda, T.; Tsutsumi, O. *Science* **1995**, *268*, 1873.
- (3) Han, M.; Ichimura, K. *Macromolecules* **2001**, *34*, 90.
- (4) Viswanathan, N. K.; Kim, D. Y.; Bian, S.; Williams, J.; Liu, W.; Li, L.; Samuelson, L.; Kumar, J.; Tripathy, S. K. *J. Mater. Chem.* **1999**, *9*, 1941.
- (5) Rasmussen, P. H.; Ramanujam, P. S.; Hvilsted, S.; Berg, R. H. *J. Am. Chem. Soc.* **1999**, *121*, 4738.

- (6) Bai, S.; Zhao, Y. *Macromolecules* **2002**, *35*, 9657.
- (7) Hagen, R.; Bieringer, T. *Adv. Mater.* **2001**, *13*, 1805.
- (8) Wu, Y.; Zhang, Q.; Kanazawa, A.; Shiono, T.; Ikeda, T.; Nagase, Y. *Macromolecules* **1999**, *32*, 3951.
- (9) Andruzzi, L.; Altomare, A.; Ciardelli, F.; Solaro, R.; Hvilsted, S.; Ramanujam, P. S. *Macromolecules* **1999**, *32*, 448.
- (10) Mao, G.; Wang, J.; Clingman, S. R.; Ober, C. K.; Chen, J. T.; Thomas, E. L. *Macromolecules* **1997**, *30*, 2556.
- (11) Walther, M.; Faulhammer, H.; Finkelmann, H. *Macromol. Chem. Phys.* **1998**, *199*, 223.
- (12) Tian, Y.; Watanabe, K.; Kong, X.; Abe, J.; Iyoda, T. *Macromolecules* **2002**, *35*, 3739.
- (13) Patten, T. E.; Xia, J.; Abernathy, T.; Matyjaszewski, K. *Science* **1996**, *272*, 866.
- (14) Anthamatten, M.; Wu, J.-S.; Hammond, P. T. *Macromolecules* **2001**, *34*, 8574.
- (15) Moriya, K.; Seki, T.; Nakagawa, M.; Mao, G.; Ober, C. K. *Macromol. Rapid Commun.* **2000**, *21*, 1309.
- (16) Ringsdorf, H.; Schmidt, H. W. *Makromol. Chem.* **1984**, *185*, 1327.
- (17) Natansohn, A.; Rochon, P.; Gosselin, J.; Xie, S. *Macromolecules* **1992**, *25*, 2268.
- (18) Krueger, H.; Wolff, D.; Aschuppe, V. *Acta Polym.* **1992**, *43*, 283.
- (19) Cloutier, S.; Peyrot, D.; Galstian, T.; Lessard, R. *J. Opt. A: Pure Appl. Opt.* **2002**, *4*, S228.
- (20) Matyjaszewski, K.; Xia, J. *Chem. Rev.* **2001**, *101*, 2921.
- (21) Kamigaito, M.; Ando, T.; Sawamoto, M. *Chem. Rev.* **2001**, *101*, 3689.
- (22) Chambard, G.; Klumperman, B.; German, A. L. *Macromolecules* **2000**, *33*, 4417.

MA0351524